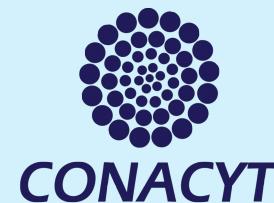


The 2022 CFNS Summer  
School on the Physics  
of Electron-Ion Collider



# Extraction fractions moments using Machine Learning techniques in $pp \rightarrow \pi + \gamma$ process

**David Francisco Rentería-Estrada**  
Universidad Autónoma de Sinaloa, México

Based on:

- 1011.0486
- 2104.14663
- 2112.05043

In colaboration with:  
**Roger J. Hernández Pinto**  
**German F.R. Sborlini**  
**Pia Zurita**

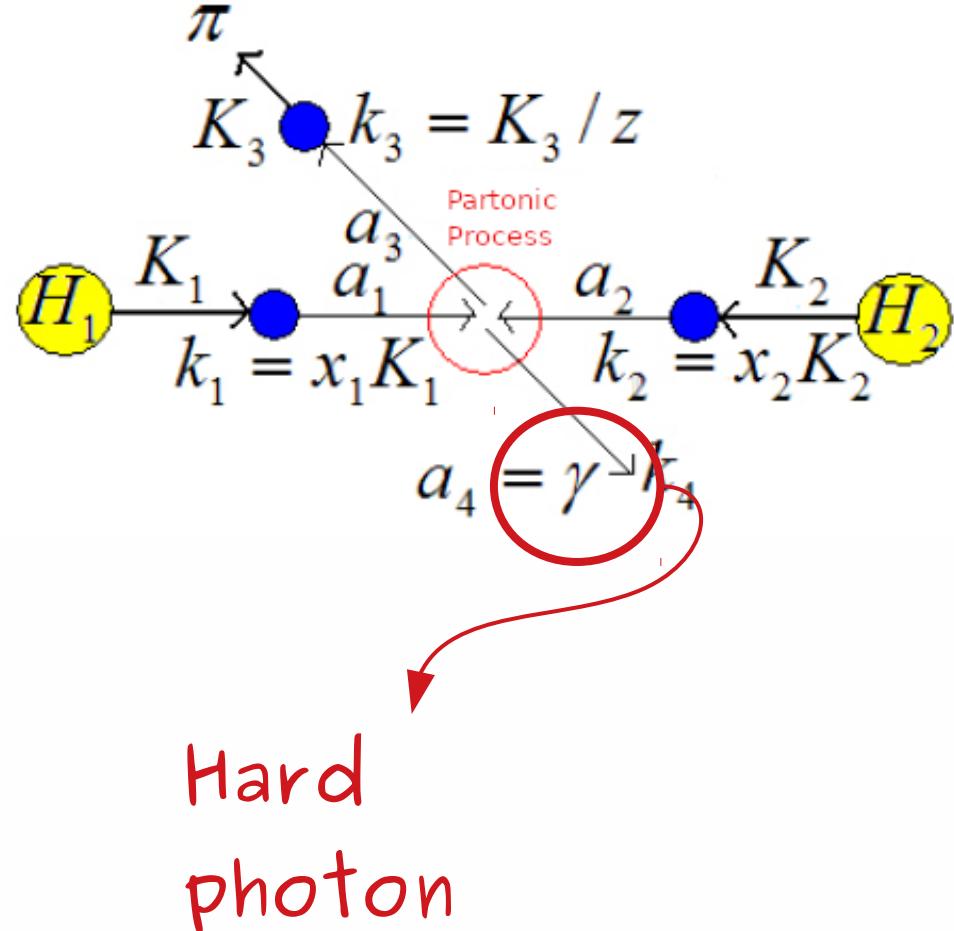
July 21<sup>th</sup>, 2022

# Process

In this work we are interested in studying the production of a direct photon plus a pion in proton-proton collision:

$$pp \rightarrow \pi^+ + \gamma$$

The aim is reconstruct the momentum fraction  $x_1$ ,  $x_2$  and  $z$  of the original partons in the interaction to NLO QCD + LO QED accuracy.



# Motivation

- Aim: reconstruct the momentum fractions  $x_1$ ,  $x_2$  and  $z$ .
- Nowadays, Machine Learning is a tool that allows to make a predictive model to reconstruct  $\{x_1, x_2, z\}$ .

1011.0486

PHYSICAL REVIEW D 83, 074022 (2011)

## Hadron plus photon production in polarized hadronic collisions at next-to-leading order accuracy

Daniel de Florian and Germán F.R. Sborlini

*Departamento de Física Facultad de Ciencias Exactas y Naturales, Universidad de Buenos Aires Pabellón I, Ciudad Universitaria (1428) Capital Federal, Argentina*

(Received 3 November 2010; revised manuscript received 23 February 2011; published 27 April 2011)

We compute the next-to-leading order QCD corrections to the polarized (and unpolarized) cross sections for the production of a hadron accompanied by an opposite-side prompt photon. This process, being studied at RHIC, permits us to reconstruct partonic kinematics using experimentally measurable variables. We study the correlation between the reconstructed momentum fractions and the true partonic ones, which in the polarized case might allow us to reveal the spin-dependent gluon distribution with a higher precision.

DOI: 10.1103/PhysRevD.83.074022

PACS numbers: 13.88.+e, 12.38.Bx, 13.87.Fh

2011

Extraction fractions moments using Machine Learning techniques in  $pp \rightarrow \pi + \gamma$  process.

2104.14663

Analysis of the internal structure of hadrons using direct photon production

David F. Rentería-Estrada,<sup>a</sup> Roger J. Hernández-Pinto<sup>a</sup> and German F. R. Sborlini<sup>b,c</sup>

*loa, Ciudad Universi-*

*ten, Germany.*

*ior de Investigaciones*

2112.05043

## Reconstructing partonic kinematics at colliders with Machine Learning

D. F. Rentería-Estrada,<sup>a</sup> R. J. Hernández-Pinto,<sup>a</sup> G. F. R. Sborlini<sup>b,c</sup> and P. Zurita<sup>d</sup>

<sup>a</sup>*Facultad de Ciencias Físico-Matemáticas, Universidad Autónoma de Sinaloa, Ciudad Universitaria, CP 80000 Culiacán, Mexico*

<sup>b</sup>*Instituto de Física Corpuscular, Universitat de València – Consejo Superior de Investigaciones Científicas, Parc Científic, E-46980 Paterna, Valencia, Spain*

<sup>c</sup>*Deutsches Elektronen-Synchrotron DESY, Platanenallee 6, 15738 Zeuthen, Germany*

<sup>d</sup>*Institut für Theoretische Physik, Universität Regensburg, 93040 Regensburg, Germany, Universität Regensburg, Germany*

*E-mail: davidrenteria.fcfm@uas.edu.mx, roger@uas.edu.mx, german.sborlini@desy.de, maria.zurita@ur.de*

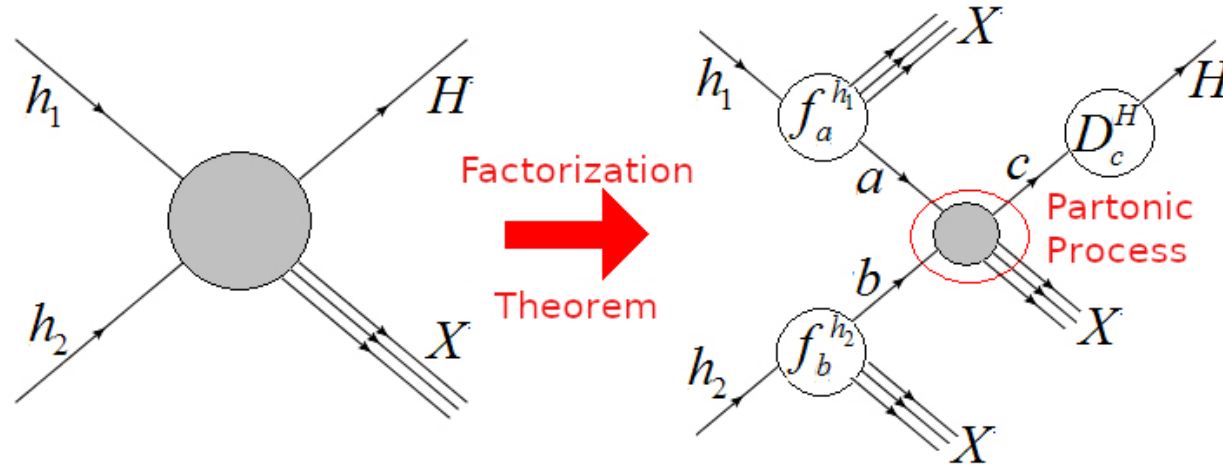
of hadrons is a hard  
is starting from first  
is necessary to use  
article, we describe  
i. Using up-to-date  
rections to hadron

2021

# Hadronic Cross-Section

In hadron-hadron collisions, the cross section is described by the convolution between PDFs, FFs, and the partonic cross section.

$$d\sigma^{h_1 h_2 \rightarrow H X} = \sum_{a,b,c} \int_0^1 dx \int_0^1 dy \int_0^1 dz f_a^{h_1}(x, \mu_I) f_b^{h_2}(y, \mu_I) d_c^H(z, \mu_F) d\hat{\sigma}_{ab \rightarrow cX}$$





# Cross section calculation

- The Cross-Section at NLO QCD is implement in FKS (virtual + real + UV counter terms + ISR counter-terms)

## Hadronic cross-section

$$d\sigma_{H_1 H_2 \rightarrow h \gamma} = \sum_{a_1, a_2, a_3} \int_0^1 dx_1 dx_2 dz f_{a_1}^{H_1}(x_1, \mu_I) f_{a_2}^{H_2}(x_2, \mu_I) d_{a_3}^h(z, \mu_F) d\hat{\sigma}_{a_1 a_2 \rightarrow a_3 \gamma}^{ISO}.$$

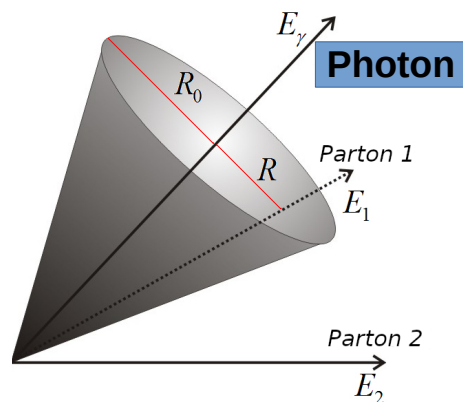
## Partonic cross-section

$$\begin{aligned} d\hat{\sigma}_{a_1 a_2 \rightarrow a_3 \gamma}^{ISO} &= \frac{\alpha_s}{2\pi} \frac{\alpha}{2\pi} \int dPS^{2 \rightarrow 2} \frac{|\mathcal{M}^{(0)}|^2(x_1 K_1, x_2 K_2, K_3/z, K_4)}{2\hat{s}} \mathcal{S}_2 \\ &+ \frac{\alpha_s^2}{4\pi^2} \frac{\alpha}{2\pi} \int dPS^{2 \rightarrow 2} \frac{|\mathcal{M}^{(1)}|^2(x_1 K_1, x_2 K_2, K_3/z, K_4)}{2\hat{s}} \mathcal{S}_2 \\ &+ \frac{\alpha_s^2}{4\pi^2} \frac{\alpha}{2\pi} \sum_{a_5} \int dPS^{2 \rightarrow 3} \frac{|\mathcal{M}^{(0)}|^2(x_1 K_1, x_2 K_2, K_3/z, K_4, k_5)}{2\hat{s}} \mathcal{S}_3 \\ d\hat{\sigma}_{a_1 a_2 \rightarrow a_3 \gamma}^{ISO, QED} &= \frac{\alpha^2}{4\pi^2} \int dPS^{2 \rightarrow 2} \frac{|\mathcal{M}_{QED}^{(0)}|^2(x_1 K_1, x_2 K_2, K_3/z, K_4)}{2\hat{s}} \mathcal{S}_2. \end{aligned}$$

LO QCD	LO QED	NLO QCD
$q\bar{q} \rightarrow \gamma g$	$q\gamma \rightarrow \gamma q$	$q\bar{q} \rightarrow \gamma g g$
$qg \rightarrow \gamma q$	$q\bar{q} \rightarrow \gamma\gamma$	$qg \rightarrow \gamma g q$
		$gg \rightarrow \gamma q\bar{q}$
		$q\bar{q} \rightarrow \gamma Q\bar{Q}$
		$qQ \rightarrow \gamma q Q$

# Computational details

The selection procedure is given by the Smooth Cone Isolation algorithm

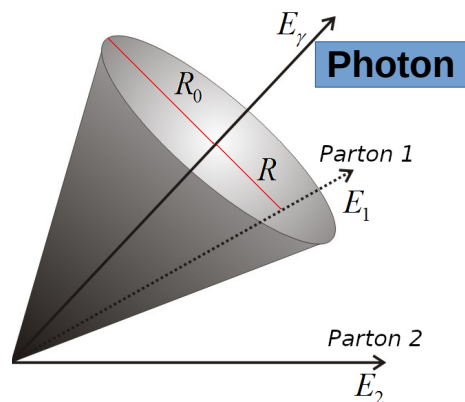


$$R = r_j = \sqrt{(\eta_j - \eta_0)^2 + (\phi_j - \phi_0)^2}$$

Smooth cone isolation

# Computational details

The selection procedure is given by the Smooth Cone Isolation algorithm



Smooth function:  $\xi(r) = \epsilon_\gamma E_T^\gamma \left( \frac{1 - \cos(r)}{1 - \cos r_0} \right)^4$

## Selection criteria

Define:  $E_T(r) = \sum_j E_{Tj} \Theta(r - r_j)$

If  $E_T(r) < \xi(r)$  Then:

$\gamma$  is Isolated

Else:

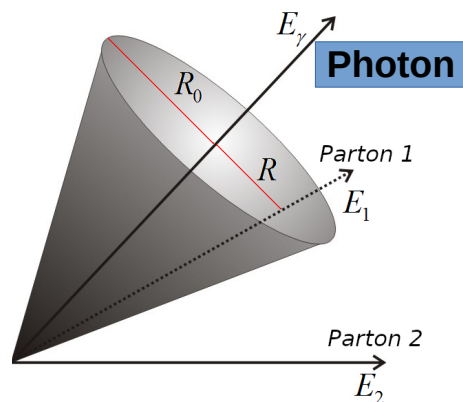
$\gamma$  is not Isolated

$$R = r_j = \sqrt{(\eta_j - \eta_0)^2 + (\phi_j - \phi_0)^2}$$

Smooth cone isolation

## Computational details

The selection procedure is given by the Smooth Cone Isolation algorithm



**Smooth function:**  $\xi(r) = \epsilon_\gamma E_T^\gamma \left( \frac{1 - \cos(r)}{1 - \cos r_0} \right)^4$

## Selection criteria

Define:  $E_T(r) = \sum_j E_{T_j} \Theta(r - r_j)$

**If  $E_T(r) < \xi(r)$  Then:**

## $\gamma$ is Isolated

Else:

## $\gamma$ is not Isolated

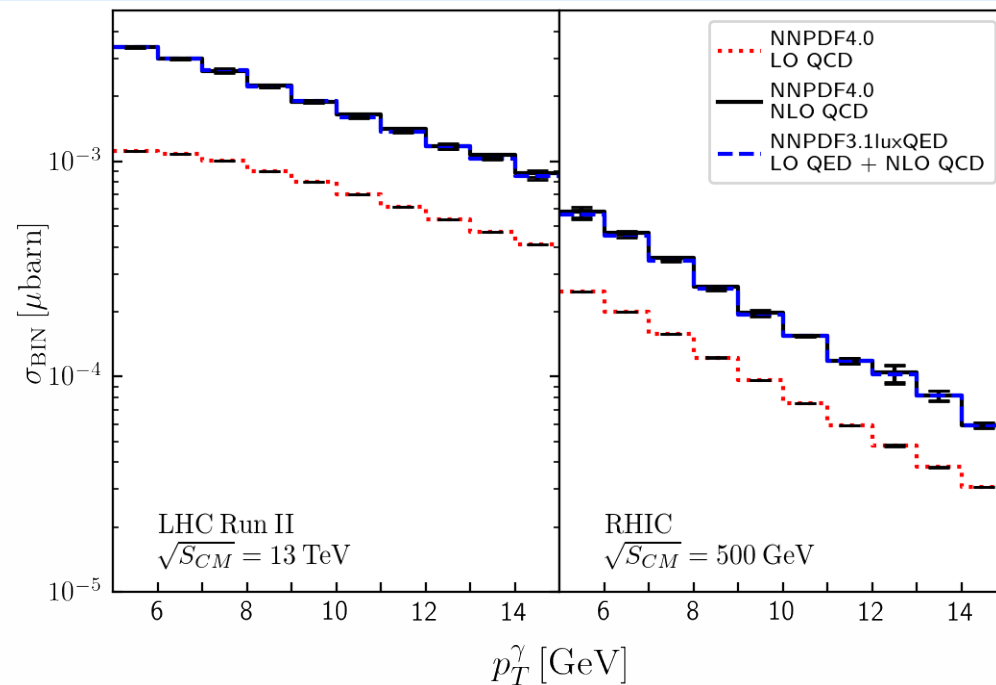
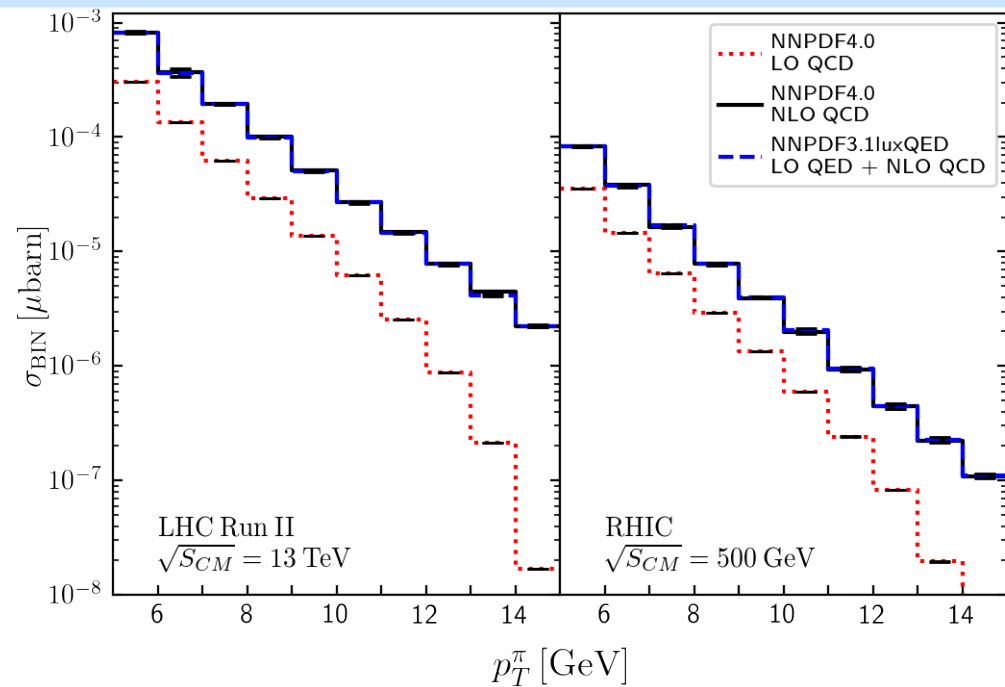
$$R = r_j = \sqrt{(\eta_j - \eta_0)^2 + (\phi_j - \phi_0)^2}$$

# Smooth cone isolation

The cuts are used by STAR/PHENIX @ RHIC

$$|\eta^h| \leq 0.35, \quad |\eta^\gamma| \leq 0.35, \quad p_T^h \geq 2 \text{ GeV}, \quad 5 \text{ GeV} \leq p_T^\gamma \leq 15 \text{ GeV}$$

# First: Photon + Hadron distributions

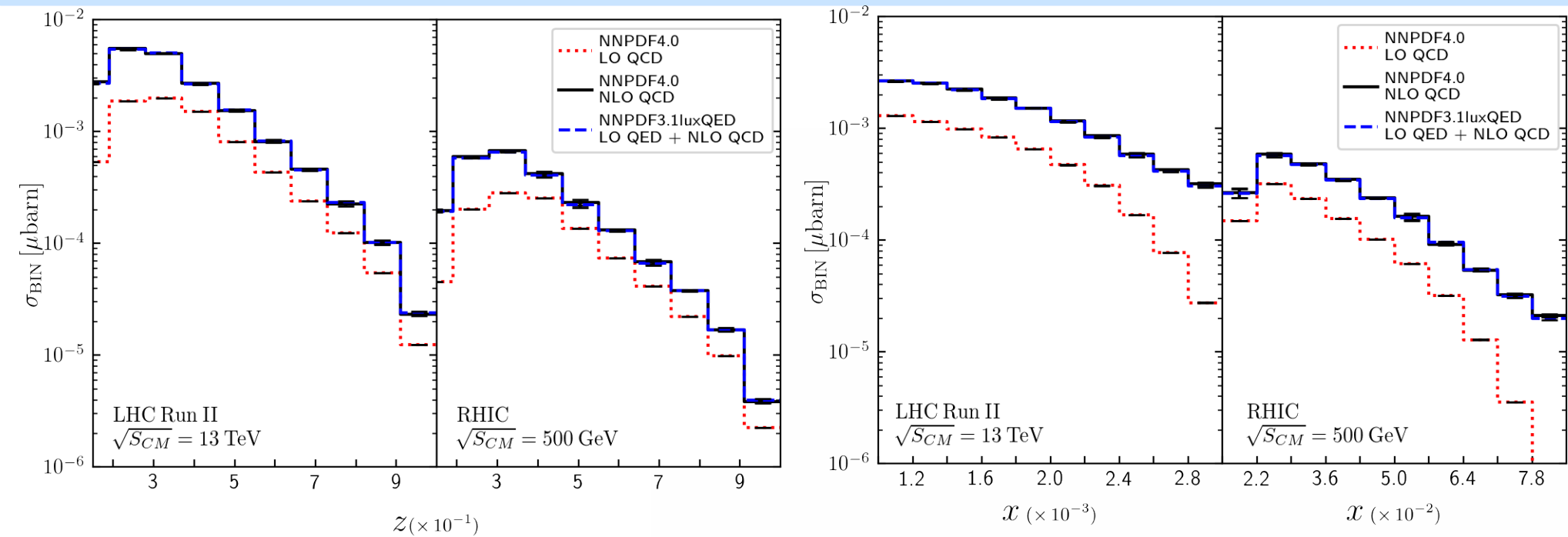


2112.05043 [hep-ph]

## Transverse momentum distribution.

- The cross-section increases for higher c.m. energies.
- The distribution in  $p_T^\pi$  falls faster than the  $p_T^\gamma$ -spectrum, mainly because of the convolution with the FFs.

# First: Photon + Hadron distributions



## Fraction momentum distribution.

2112.05043 [hep-ph]

- Important NLO QCD corrections, but small percent-level LO QED ones.
- The experimental cut in  $p_T^\gamma$  induces a restriction on the maximum value of  $\mathbf{x}$  involved in the collision.
- The distribution present a peak, located at  $\mathbf{z}_{\text{Peak}} \approx 0.35$  for RHIC  $\mathbf{z}_{\text{Peak}} \approx 0.25$  for LHC Run II.

# Reconstructing the partonic kinematics

Experimentally accessible quantities:

$$\bar{\mathcal{V}}_{\text{Exp}} = \{\bar{p}_T^\gamma, \bar{p}_T^\pi, \bar{\eta}^\gamma, \bar{\eta}^\pi, \overline{\cos}(\phi^\pi - \phi^\gamma)\} \longleftarrow \text{Detector measurements}$$

**LO kinematics**

$$x_{1,2} = \frac{p_T^\gamma}{\sqrt{s}} \left( e^{\eta^{\pm\pi}} + e^{\eta^{\pm\gamma}} \right) \quad z = \frac{p_T^\pi}{p_T^\gamma}$$

# Reconstructing the partonic kinematics

Experimentally accessible quantities:

$$\bar{\mathcal{V}}_{\text{Exp}} = \{\bar{p}_T^\gamma, \bar{p}_T^\pi, \bar{\eta}^\gamma, \bar{\eta}^\pi, \overline{\cos}(\phi^\pi - \phi^\gamma)\} \longleftarrow$$

Detector measurements

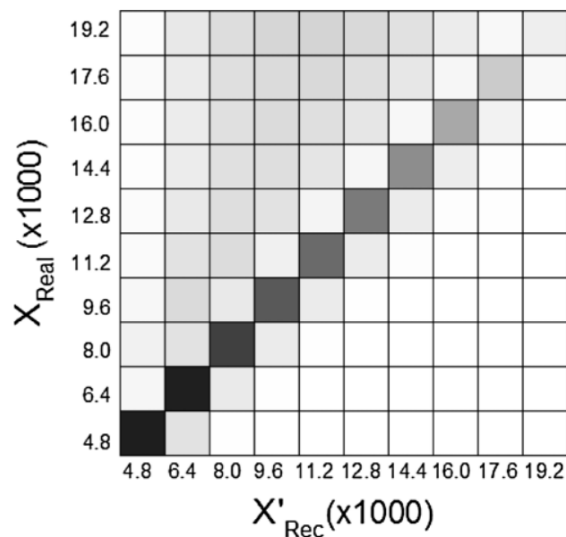
LO kinematics

$$x_{1,2} = \frac{p_T^\gamma}{\sqrt{s}} \left( e^{\eta^{\pm\pi}} + e^{\eta^{\mp\gamma}} \right) \quad z = \frac{p_T^\pi}{p_T^\gamma}$$

NLO QCD approximation (2011)

$$X_{1,\text{REC}} = \frac{p_T^\gamma \exp(\eta^\pi) - \cos(\phi^\pi - \phi^\gamma) p_T^\gamma \exp(\eta^\gamma)}{\sqrt{S_{CM}}}$$

$$X_{2,\text{REC}} = \frac{p_T^\gamma \exp(-\eta^\pi) - \cos(\phi^\pi - \phi^\gamma) p_T^\gamma \exp(-\eta^\gamma)}{\sqrt{S_{CM}}}$$





# Reconstructing the partonic kinematics

Experimentally accessible quantities:

$$\bar{\mathcal{V}}_{\text{Exp}} = \{\bar{p}_T^\gamma, \bar{p}_T^\pi, \bar{\eta}^\gamma, \bar{\eta}^\pi, \overline{\cos}(\phi^\pi - \phi^\gamma)\} \longleftarrow$$

Detector measurements

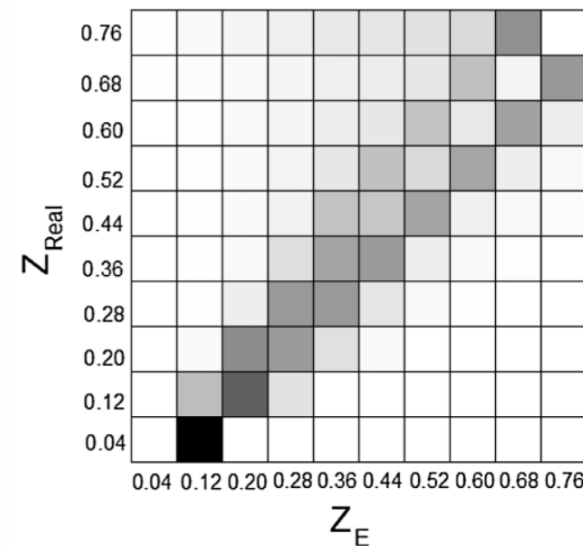
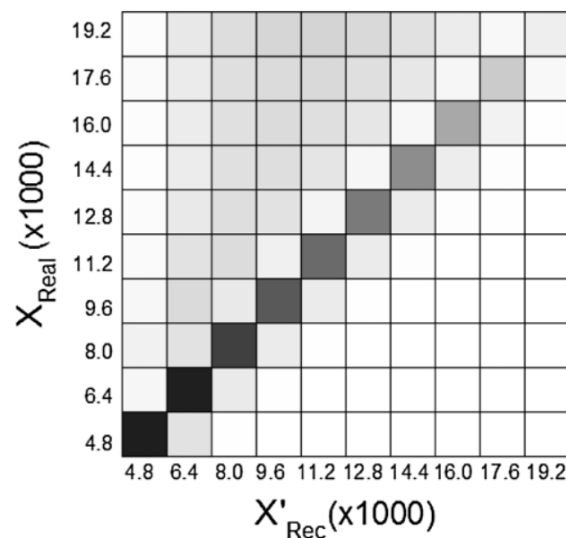
LO kinematics

$$x_{1,2} = \frac{p_T^\gamma}{\sqrt{s}} \left( e^{\eta^{\pm\pi}} + e^{\eta^{\mp\gamma}} \right) \quad z = \frac{p_T^\pi}{p_T^\gamma}$$

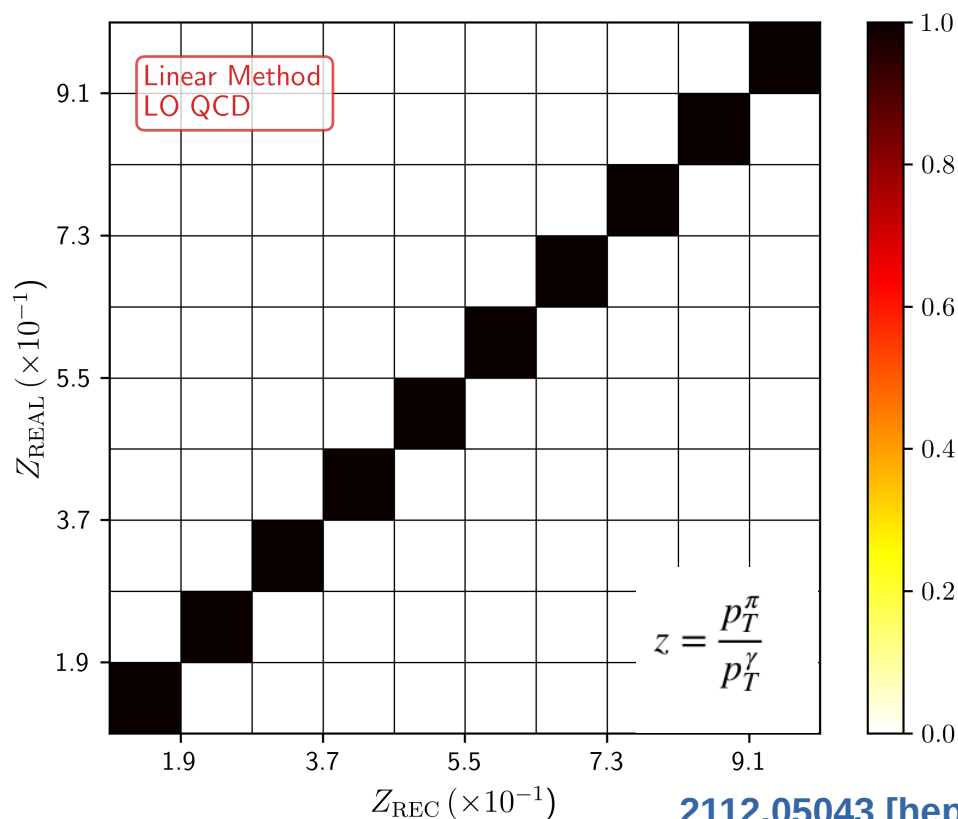
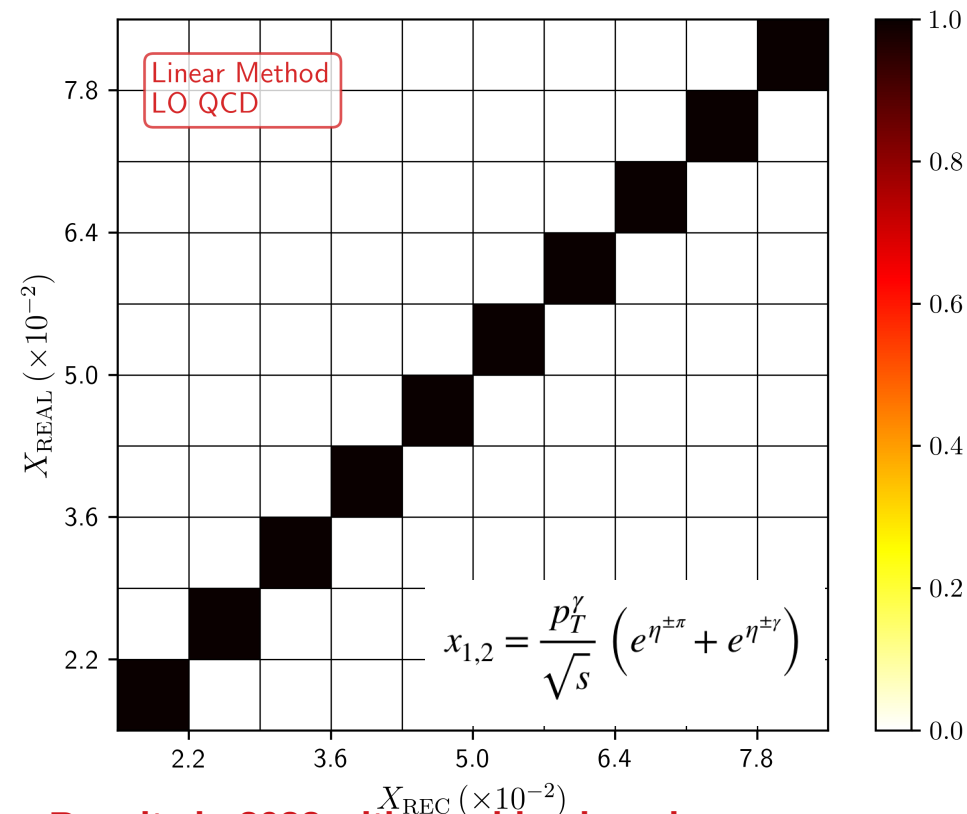
NLO QCD approximation (2011)

$$X_{1,\text{REC}} = \frac{p_T^\gamma \exp(\eta^\pi) - \cos(\phi^\pi - \phi^\gamma) p_T^\gamma \exp(\eta^\gamma)}{\sqrt{S_{CM}}}$$

$$X_{2,\text{REC}} = \frac{p_T^\gamma \exp(-\eta^\pi) - \cos(\phi^\pi - \phi^\gamma) p_T^\gamma \exp(-\eta^\gamma)}{\sqrt{S_{CM}}}$$



# Reconstructing the partonic kinematics



**Results in 2022 with machine learning.**

- We started with LO cross-sections, and applied linear regression.
- We used the basis:  $\mathcal{B}_{\text{LO}} = \left\{ \frac{p_T^\gamma}{\sqrt{S_{CM}}} \exp(\eta^\pi), \frac{p_T^\gamma}{\sqrt{S_{CM}}} \exp(\eta^\gamma), \frac{p_T^\gamma}{\sqrt{S_{CM}}} \exp(-\eta^\pi), \frac{p_T^\gamma}{\sqrt{S_{CM}}} \exp(-\eta^\gamma), p_T^\pi/p_T^\gamma \right\}$

2112.05043 [hep-ph]

# Reconstructions Methods

$$X = \{ X_{general}, X_{LO-ins}, X_{physically} \}$$

- **Linear Method**

$$Y_{REC} = \sum_{i=k}^{i=0} \alpha_i x_i \text{ for } x_i \in X_j$$
$$j = \text{general, LO-ins, physically}$$

- **Gaussian Process Regression**

$$Y_{REC} = \prod_i \exp(-||x - \mu_i||^2 / 2l^2)$$

# Reconstructions Methods

$$X = \{ X_{general}, X_{LO-ins}, X_{physically} \}$$

- Linear Method**

$$Y_{REC} = \sum_{i=k}^{i=0} \alpha_i x_i \text{ for } x_i \in X_j$$

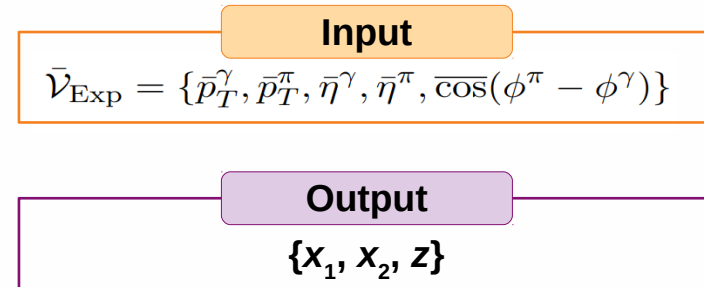
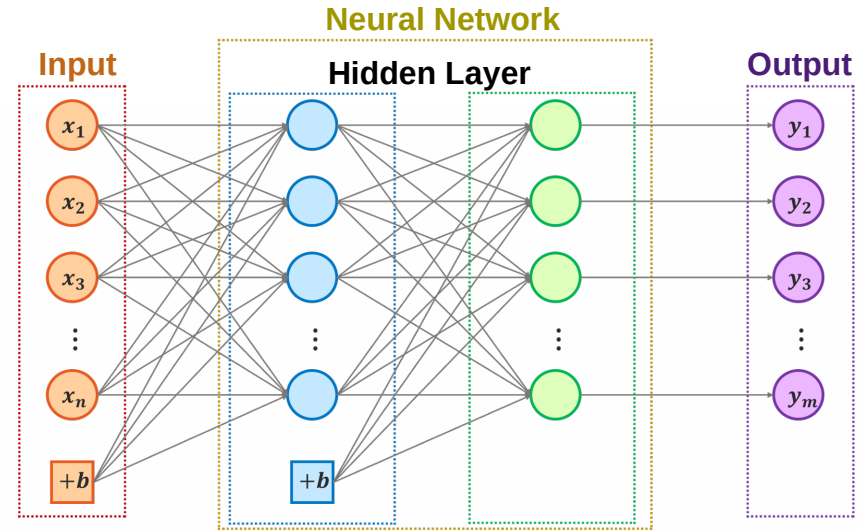
$$j = \text{general, LO-ins, physically}$$

- Gaussian Process Regression**

$$Y_{REC} = \prod_i \exp(-||x - \mu_i||^2 / 2l^2)$$

- Neural Network**

The NN implemented in this work is a **Multilayer Perceptron** with 5 hidden layers, 300 neurons per layer and a Relu (Unitary Linear Rectifier) activation function.



# Reconstructing the partonic kinematics

## General basis:

$$\mathcal{K} = \left\{ \frac{p_T^\gamma}{\sqrt{S_{CM}}}, \frac{p_T^\pi}{\sqrt{S_{CM}}}, \exp(\eta^\gamma), \exp(\eta^\pi), \cos(\phi^\pi - \phi^\gamma), \left(\frac{p_T^\gamma}{\sqrt{S_{CM}}}\right)^{-1}, \left(\frac{p_T^\pi}{\sqrt{S_{CM}}}\right)^{-1}, (\exp(\eta^\gamma))^{-1}, (\exp(\eta^\pi))^{-1} \right\}$$
$$Y_{\text{REC}} = \sum_{i=1, i \neq 5}^9 (a_i^Y + b_i^Y \mathcal{K}_5) \mathcal{K}_i + \sum_{i \leq j, \{i,j\} \neq 5, j-i \neq 5} (c_{ij}^Y + d_{ij}^Y \mathcal{K}_5) \mathcal{K}_i \mathcal{K}_j$$

# Reconstructing the partonic kinematics

## General basis:

$$\mathcal{K} = \left\{ \frac{p_T^\gamma}{\sqrt{S_{CM}}}, \frac{p_T^\pi}{\sqrt{S_{CM}}}, \exp(\eta^\gamma), \exp(\eta^\pi), \cos(\phi^\pi - \phi^\gamma), \left(\frac{p_T^\gamma}{\sqrt{S_{CM}}}\right)^{-1}, \left(\frac{p_T^\pi}{\sqrt{S_{CM}}}\right)^{-1}, (\exp(\eta^\gamma))^{-1}, (\exp(\eta^\pi))^{-1} \right\}$$
$$Y_{\text{REC}} = \sum_{i=1, i \neq 5}^9 (a_i^Y + b_i^Y \mathcal{K}_5) \mathcal{K}_i + \sum_{i \leq j, \{i, j\} \neq 5, j-i \neq 5} (c_{ij}^Y + d_{ij}^Y \mathcal{K}_5) \mathcal{K}_i \mathcal{K}_j$$

## LO-inspired basis:

$$\mathcal{B}_{\text{NLO}}^{X_1} = \left\{ \frac{p_T^\gamma}{\sqrt{S_{CM}}} \exp(\eta^\gamma), \frac{p_T^\gamma}{\sqrt{S_{CM}}} \exp(\eta^\pi), \frac{p_T^\pi}{\sqrt{S_{CM}}} \exp(\eta^\gamma), \frac{p_T^\pi}{\sqrt{S_{CM}}} \exp(\eta^\pi), \right.$$
$$\left. \frac{p_T^\gamma \mathcal{K}_5}{\sqrt{S_{CM}}} \exp(\eta^\gamma), \frac{p_T^\gamma \mathcal{K}_5}{\sqrt{S_{CM}}} \exp(\eta^\pi), \frac{p_T^\pi \mathcal{K}_5}{\sqrt{S_{CM}}} \exp(\eta^\gamma), \frac{p_T^\pi \mathcal{K}_5}{\sqrt{S_{CM}}} \exp(\eta^\pi) \right\}$$
$$\mathcal{B}_{\text{NLO}}^Z = \{ p_T^\pi / p_T^\gamma, \mathcal{K}_5 p_T^\pi / p_T^\gamma, \mathcal{K}_5 p_T^\pi / \sqrt{S_{CM}}, \mathcal{K}_5 \sqrt{S_{CM}} / p_T^\gamma \}$$

$$x_{1,2} = \frac{p_T^\gamma}{\sqrt{s}} \left( e^{\eta^{\pm\pi}} + e^{\eta^{\pm\gamma}} \right) \quad z = \frac{p_T^\pi}{p_T^\gamma}$$

# Reconstructing the partonic kinematics

## General basis:

$$\mathcal{K} = \left\{ \frac{p_T^\gamma}{\sqrt{S_{CM}}}, \frac{p_T^\pi}{\sqrt{S_{CM}}}, \exp(\eta^\gamma), \exp(\eta^\pi), \cos(\phi^\pi - \phi^\gamma), \left(\frac{p_T^\gamma}{\sqrt{S_{CM}}}\right)^{-1}, \left(\frac{p_T^\pi}{\sqrt{S_{CM}}}\right)^{-1}, (\exp(\eta^\gamma))^{-1}, (\exp(\eta^\pi))^{-1} \right\}$$

$$Y_{\text{REC}} = \sum_{i=1, i \neq 5}^9 (a_i^Y + b_i^Y \mathcal{K}_5) \mathcal{K}_i + \sum_{i \leq j, \{i, j\} \neq 5, j-i \neq 5} (c_{ij}^Y + d_{ij}^Y \mathcal{K}_5) \mathcal{K}_i \mathcal{K}_j$$

## LO-inspired basis:

$$\mathcal{B}_{\text{NLO}}^{X_1} = \left\{ \frac{p_T^\gamma}{\sqrt{S_{CM}}} \exp(\eta^\gamma), \frac{p_T^\gamma}{\sqrt{S_{CM}}} \exp(\eta^\pi), \frac{p_T^\pi}{\sqrt{S_{CM}}} \exp(\eta^\gamma), \frac{p_T^\pi}{\sqrt{S_{CM}}} \exp(\eta^\pi), \right.$$

$$\left. \frac{p_T^\gamma \mathcal{K}_5}{\sqrt{S_{CM}}} \exp(\eta^\gamma), \frac{p_T^\gamma \mathcal{K}_5}{\sqrt{S_{CM}}} \exp(\eta^\pi), \frac{p_T^\pi \mathcal{K}_5}{\sqrt{S_{CM}}} \exp(\eta^\gamma), \frac{p_T^\pi \mathcal{K}_5}{\sqrt{S_{CM}}} \exp(\eta^\pi) \right\}$$

$$\mathcal{B}_{\text{NLO}}^Z = \{ p_T^\pi / p_T^\gamma, \mathcal{K}_5 p_T^\pi / p_T^\gamma, \mathcal{K}_5 p_T^\pi / \sqrt{S_{CM}}, \mathcal{K}_5 \sqrt{S_{CM}} / p_T^\gamma \}$$

## Physically-motivated basis

$$x_{1,2} = \frac{p_T^\gamma}{\sqrt{s}} \left( e^{\eta^{\pm\pi}} + e^{\eta^{\pm\gamma}} \right)$$

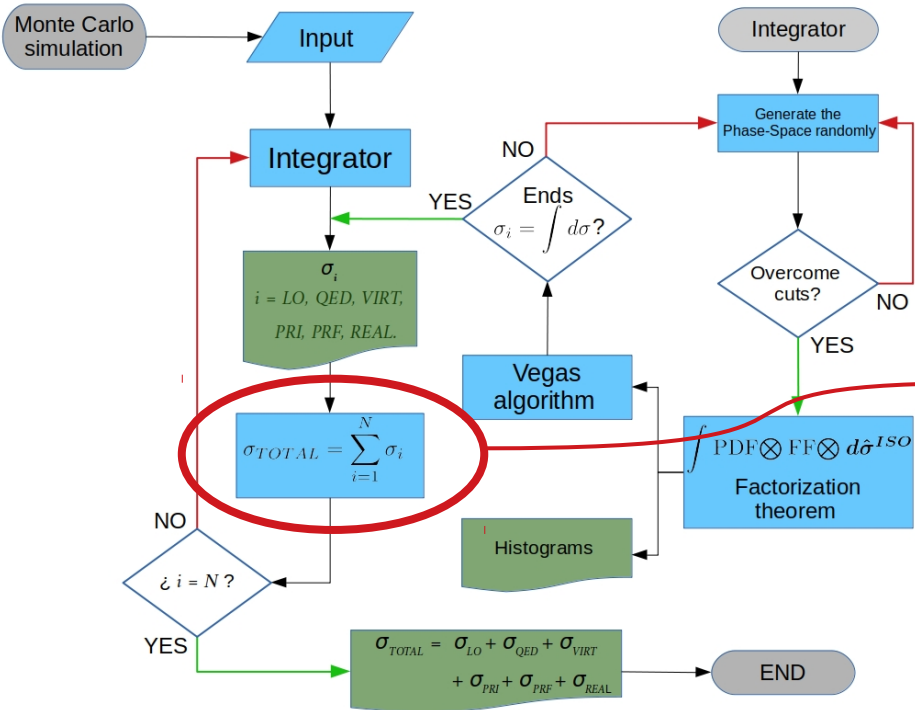
$$z = \frac{p_T^\pi}{p_T^\gamma}$$

$$b_6^{X_1} = 0, \\ c_{6,j}^{X_1} = d_{6,j}^{X_1} = c_{i,6}^{X_1} = d_{i,6}^{X_1} = 0 \quad \{i, j\} \in \{1, \dots, 9\},$$

$$b_1^Z = b_7^Z = 0, \\ c_{1,j}^Z = d_{1,j}^Z = 0 \quad j \in \{1, \dots, 9\}, j \neq \{5, 7\}, \\ c_{i,7}^Z = d_{i,7}^Z = 0 \quad i \in \{1, \dots, 9\}, i \neq \{1, 5\},$$

# Reconstructing the partonic kinematics

## Reconstructing $\{x, z\}$ at higher-order



- NLO corrections involve: real (2-to-3), virtual (2-to-2), counterterms (2-to-2).

- Create “bins” in the external variables and compute the cross-section:

$$p_j = \{\bar{p}_T^\gamma, \bar{p}_T^\pi, \bar{\eta}^\gamma, \bar{\eta}^\pi, \overline{\cos}(\phi^\pi - \phi^\gamma)\} \in \bar{\mathcal{V}}_{\text{Exp}}$$

$$\sigma_j(\bar{p}_T^\gamma, \bar{p}_T^\pi, \bar{\eta}^\gamma, \bar{\eta}^\pi, \overline{\cos}(\phi^\pi - \phi^\gamma)) = \int_{(p_T^\gamma)_{j,\text{MIN}}}^{(p_T^\gamma)_{j,\text{MAX}}} dp_T^\gamma \int_{(p_T^\pi)_{j,\text{MIN}}}^{(p_T^\pi)_{j,\text{MAX}}} dp_T^\pi \dots \times \int dx_1 dx_2 dz d\bar{\sigma}$$

- Weight the MC momentum fractions with the cross-section per bin:

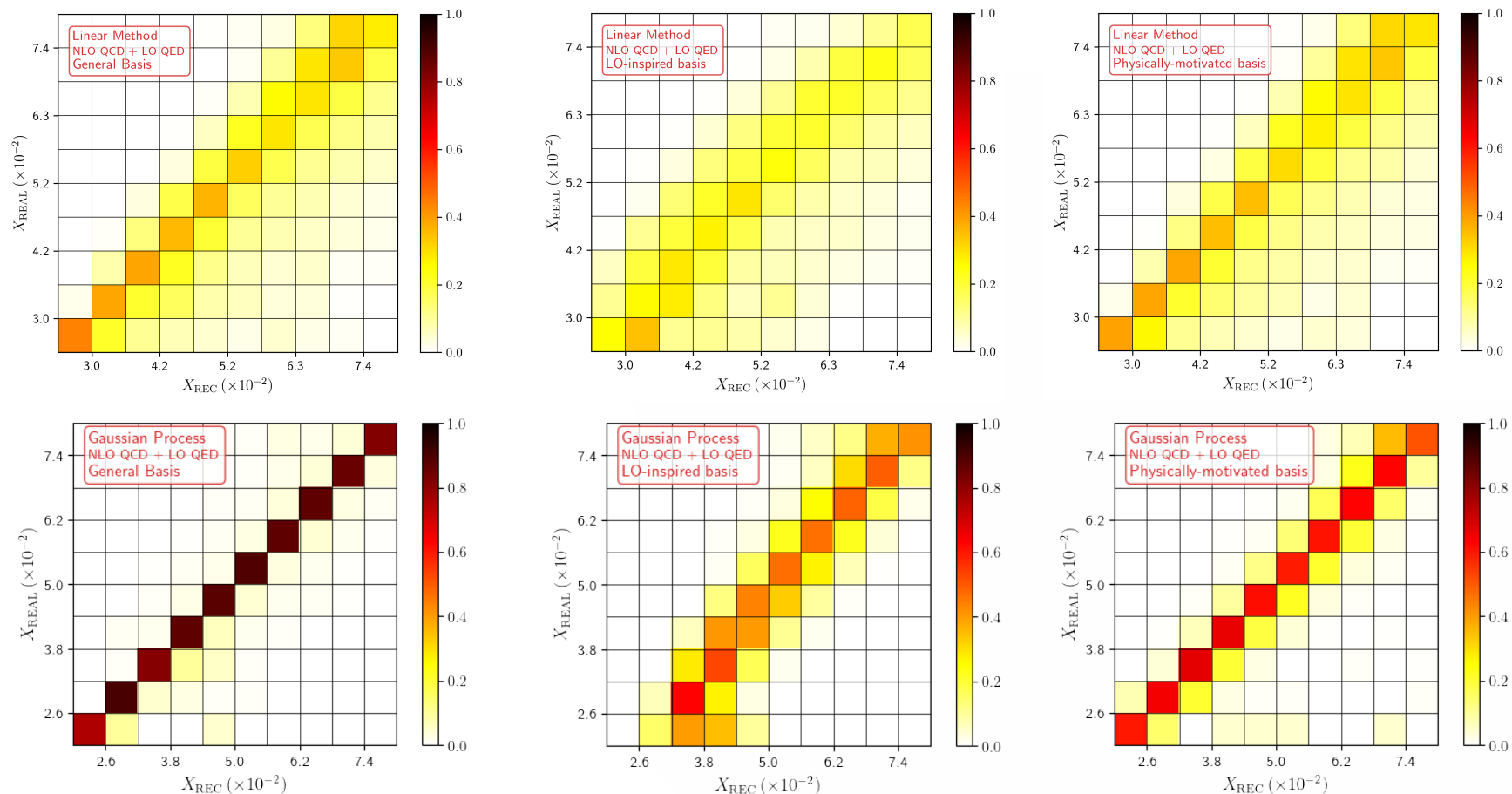
$$(x_1)_j = \sum_i (x_1)_i \frac{d\sigma_j}{dx_1}(p_j; (x_1)_i)$$

$$(z)_j = \sum_i z_i \frac{d\sigma_j}{dz}(p_j; z_i)$$



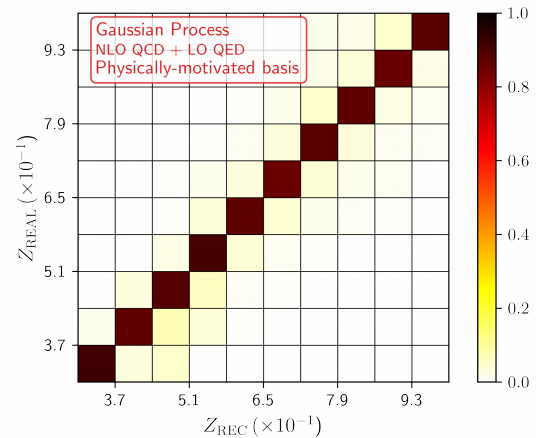
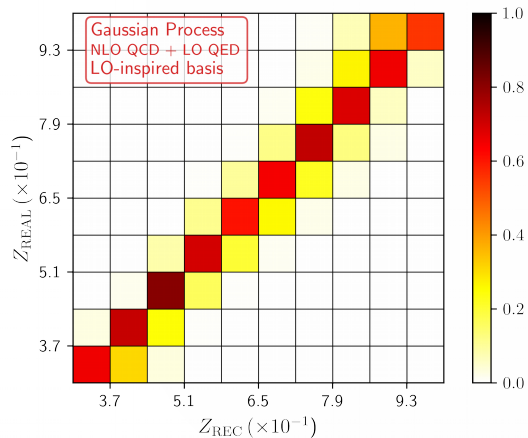
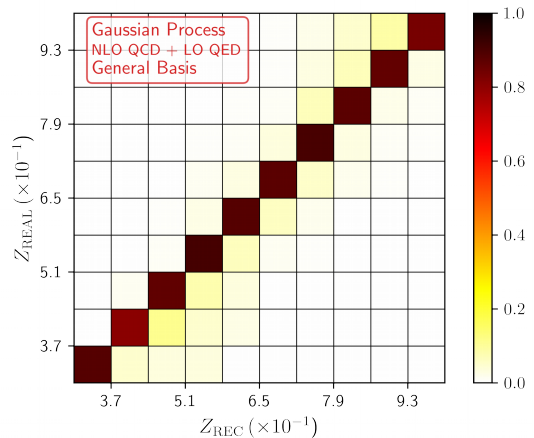
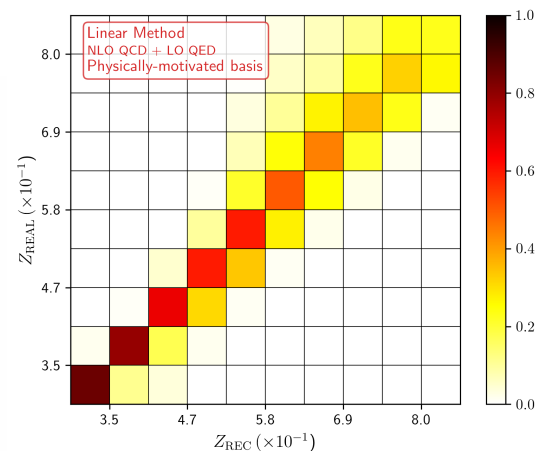
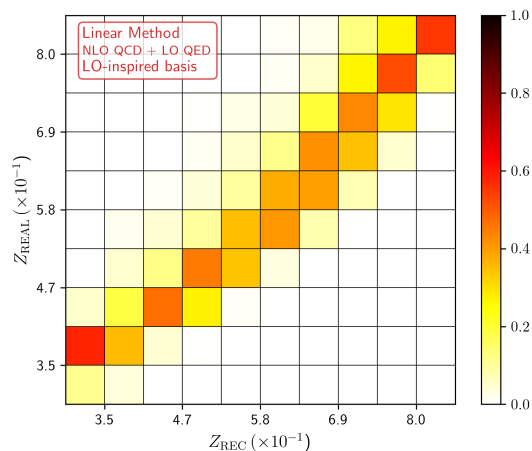
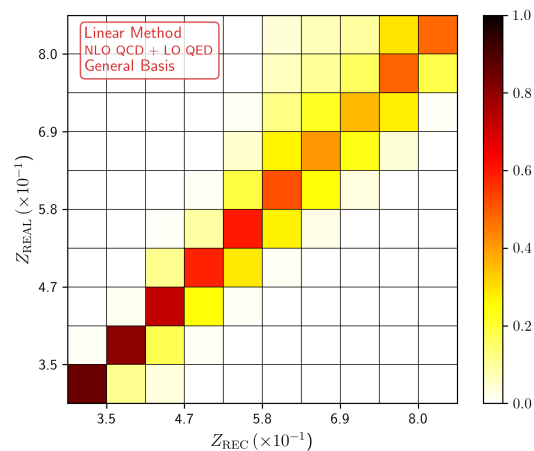
# Reconstructing the partonic kinematics

2112.05043 [hep-ph]

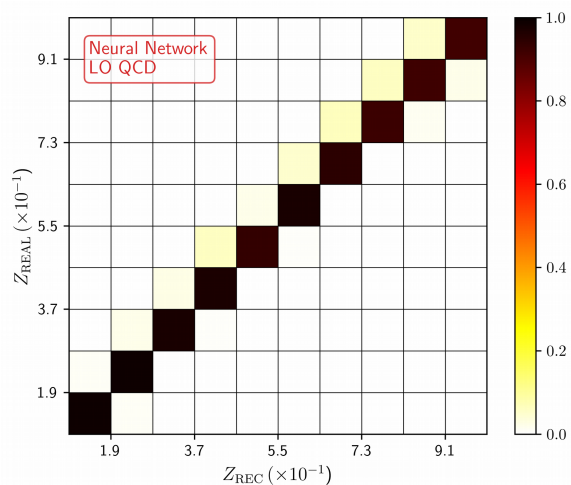
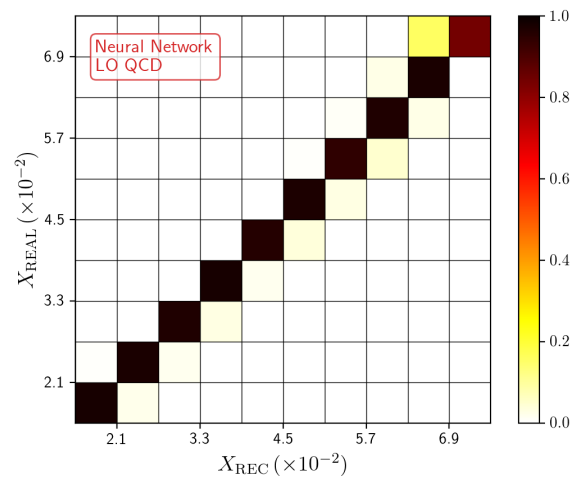


# Reconstructing the partonic kinematics

2112.05043 [hep-ph]

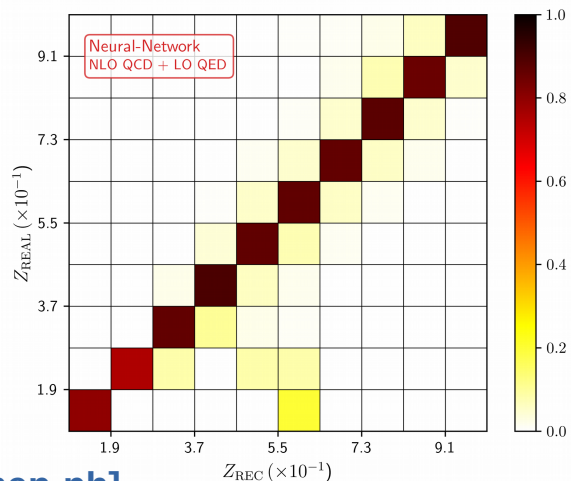
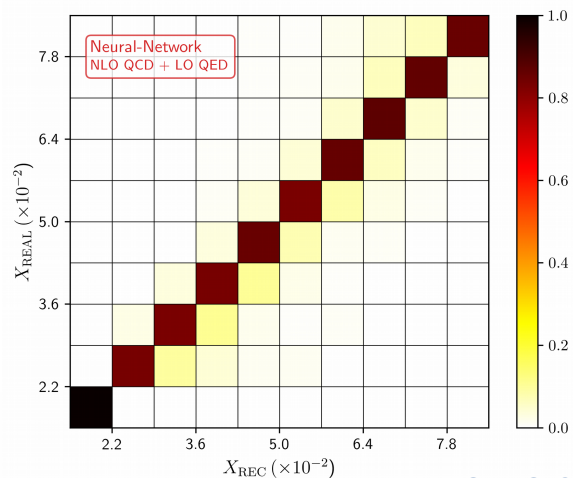


# Reconstructing the partonic kinematics



**Neural Networks (NN)  
reconstruction**

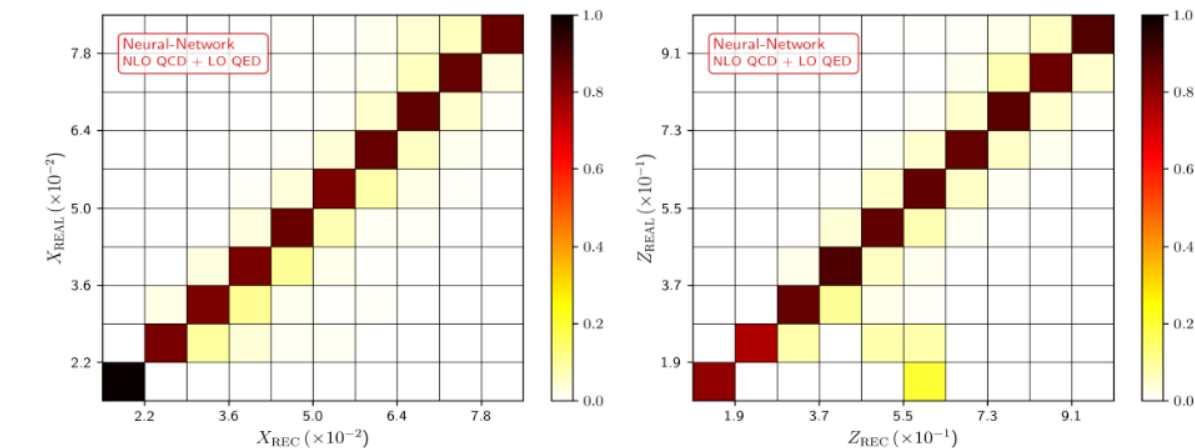
**LO prediction**



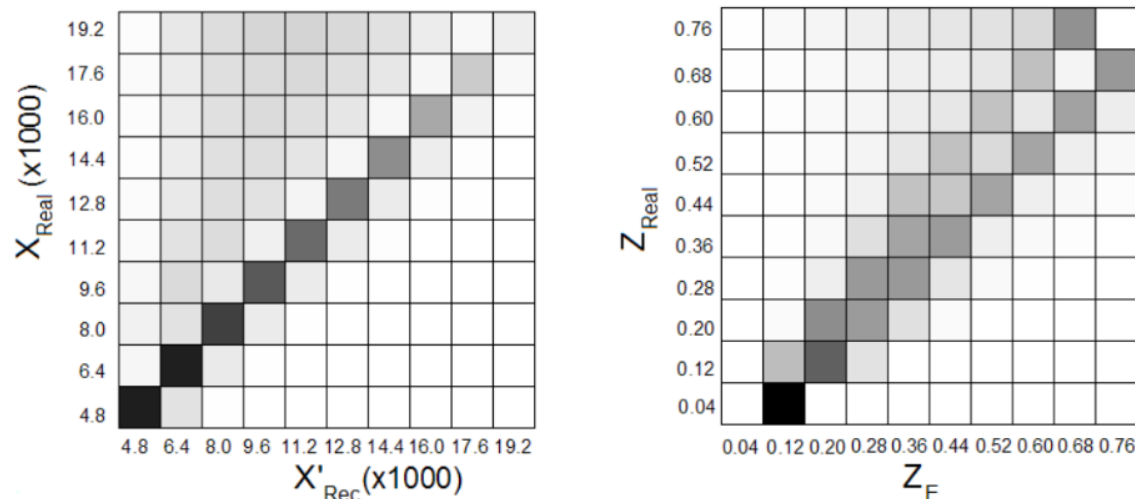
**NLO QCD + LO QED  
prediction**

2112.05043 [hep-ph]

# Reconstructing the partonic kinematics



arXiv:2112.05043 [hep-ph]  
Machine Learning  
2022



arXiv:1011.0486 [hep-ph]  
Analytical formula approx  
2011

# Conclusions

- Updated results are still consistent with '11 analysis (modifications come from new PDFs and better FFs)
- **LM**: better for large-size basis
- **GR**: has more flexibility, and better agreement w.r.t. LM (improvement in X)
- **NN**: based on MLP, offers the best balance between assumptions and quality of the reconstruction

MLP techniques (specially NN) offers an outstanding framework to understand the partonic kinematics in an (almost) automatized and (almost) human-independent way

# Conclusions

- Updated results are still consistent with '11 analysis (modifications come from new PDFs and better FFs)
- **LM**: better for large-size basis
- **GR**: has more flexibility, and better agreement w.r.t. LM (improvement in X)
- **NN**: based on MLP, offers the best balance between assumptions and quality of the reconstruction

**MLP techniques (specially NN) offers an outstanding framework to understand the partonic kinematics in an (almost) automatized and (almost) human-independent way**



**Thanks!**

# Motivation

- Aim: reconstruct the momentum fractions  $x_1$ ,  $x_2$  and  $z$ .
- Nowadays, Machine Learning is a tool that allows to make a predictive model to reconstruct  $\{x_1, x_2, z\}$ .

1011.0486

PHYSICAL REVIEW D 83, 074022 (2011)

## Hadron plus photon production in polarized hadronic collisions at next-to-leading order accuracy

Daniel de Florian and Germán F.R. Sborlini

*Departamento de Física Facultad de Ciencias Exactas y Naturales, Universidad de Buenos Aires Pabellón I, Ciudad Universitaria (1428) Capital Federal, Argentina*

(Received 3 November 2010; revised manuscript received 23 February 2011; published 27 April 2011)

We compute the next-to-leading order QCD corrections to the polarized (and unpolarized) cross sections for the production of a hadron accompanied by an opposite-side prompt photon. This process, being studied at RHIC, permits us to reconstruct partonic kinematics using experimentally measurable variables. We study the correlation between the reconstructed momentum fractions and the true partonic ones, which in the polarized case might allow us to reveal the spin-dependent gluon distribution with a higher precision.

DOI: 10.1103/PhysRevD.83.074022

PACS numbers: 13.88.+e, 12.38.Bx, 13.87.Fh

2104.14663

Analysis of the internal structure of hadrons using direct photon production

David F. Rentería-Estrada,<sup>a</sup> Roger J. Hernández-Pinto<sup>a</sup> and German F. R. Sborlini<sup>b,c</sup>

*loa, Ciudad Universi-*

*ten, Germany.*

*ior de Investigaciones*

2112.05043

## Reconstructing partonic kinematics at colliders with Machine Learning

D. F. Rentería-Estrada,<sup>a</sup> R. J. Hernández-Pinto,<sup>a</sup> G. F. R. Sborlini<sup>b,c</sup> and P. Zurita<sup>d</sup>

<sup>a</sup>*Facultad de Ciencias Físico-Matemáticas, Universidad Autónoma de Sinaloa, Ciudad Universitaria, CP 80000 Culiacán, Mexico*

<sup>b</sup>*Instituto de Física Corpuscular, Universitat de València – Consejo Superior de Investigaciones Científicas, Parc Científic, E-46980 Paterna, Valencia, Spain*

<sup>c</sup>*Deutsches Elektronen-Synchrotron DESY, Platanenallee 6, 15738 Zeuthen, Germany*

<sup>d</sup>*Institut für Theoretische Physik, Universität Regensburg, 93040 Regensburg, Germany, Universität Regensburg, Germany*

*E-mail: davidrenteria.fcfm@uas.edu.mx, roger@uas.edu.mx, german.sborlini@desy.de, maria.zurita@ur.de*

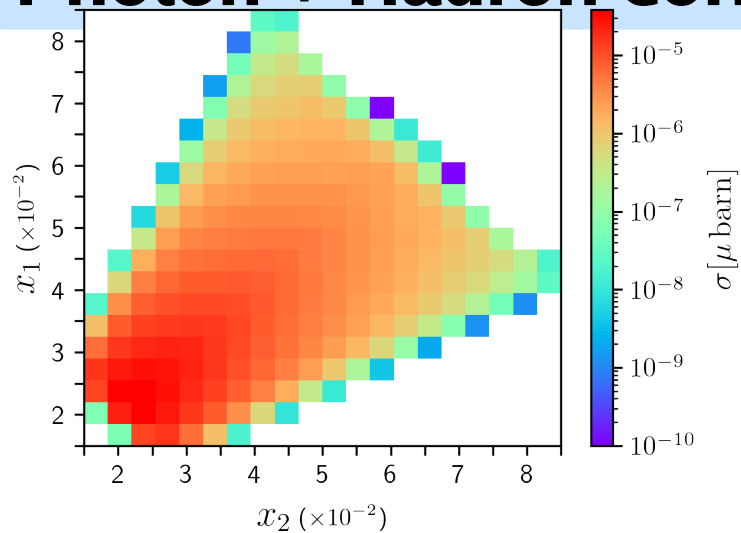
of hadrons is a hard  
is starting from first  
is necessary to use  
article, we describe  
i. Using up-to-date  
rections to hadron

2011

2021

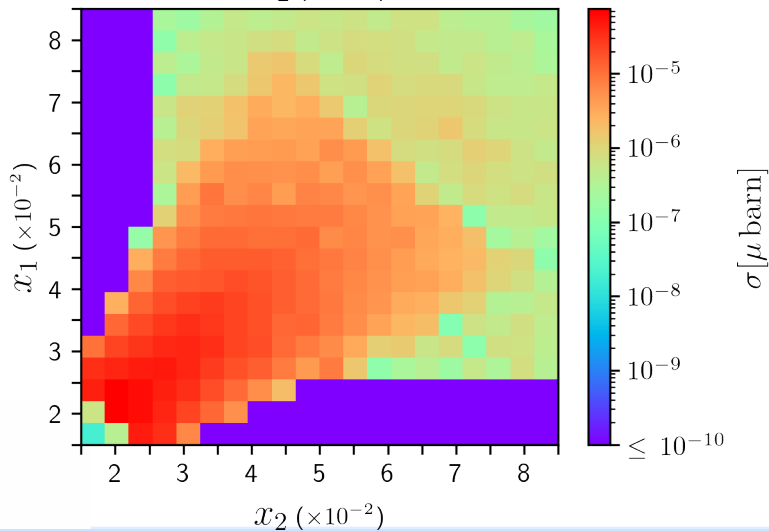


# Photon + Hadron correlations



LO QCD

- Positive correlation
- Consequence of the initial state symmetry (pp collision)
- It is a cross-check



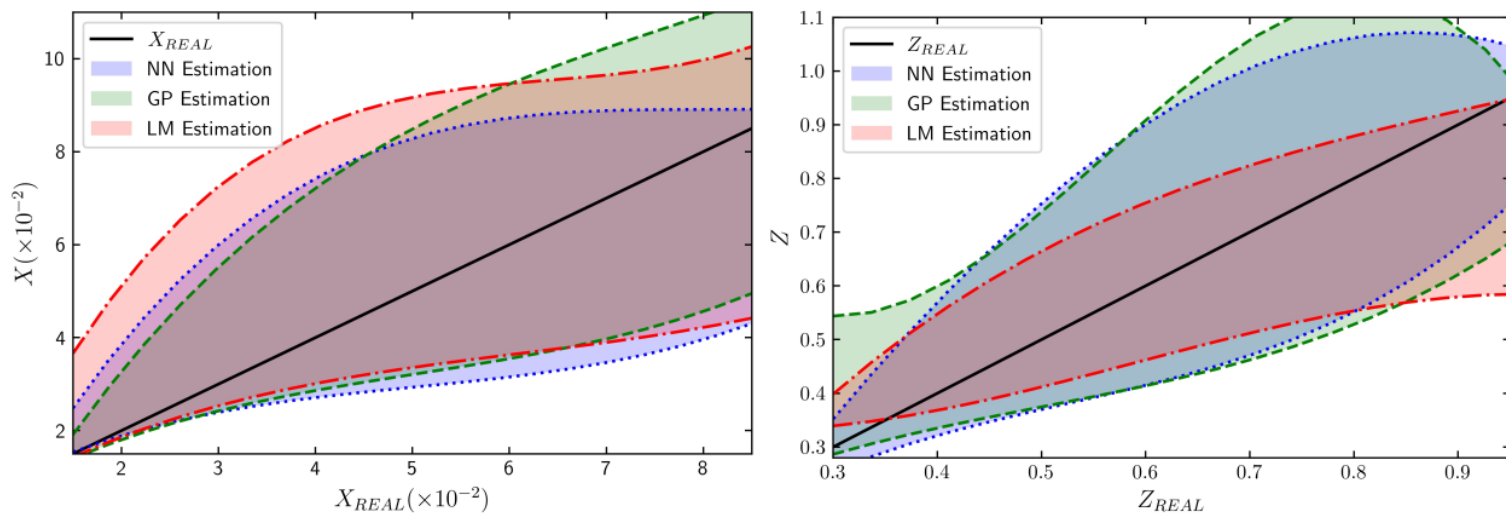
NLO QCD + LO QED

This procedure leads to three functions for reconstructing each momentum fraction: given a kinematic point in the grid,  $p_j \in \bar{\mathcal{V}}_{\text{Exp}}$ , we have

$$X(p_j) \equiv \{X_{\text{REC}}^{(\xi=2)}(p_j), X_{\text{REC}}^{(\xi=1)}(p_j), X_{\text{REC}}^{(\xi=1/2)}(p_j)\}, \quad (50)$$

and define

$$X_{\text{REC}}(p_j) = \overline{X(p_j)} \pm \frac{\max(X(p_j)) - \min(X(p_j))}{2} \equiv \overline{X(p_j)} \pm \Delta X(p_j), \quad (51)$$



Parameters	TEST 1	TEST 2	TEST 3
# hidden layers	2	4	3
# neurons/layer	50	100	100
tolerance	$10^{-2}$	$10^{-2}$	$10^{-3}$
max. number of iterations	$10^8$	$10^8$	$10^9$
# iterations w/o change	14,000	21,000	100,000

Table 3: Architectures for the MLP of three different tests for the reconstruction of the momentum fractions at NLO in QCD. All parameters are taken to be the same for  $X_{\text{REC}}$  and  $Z_{\text{REC}}$ .

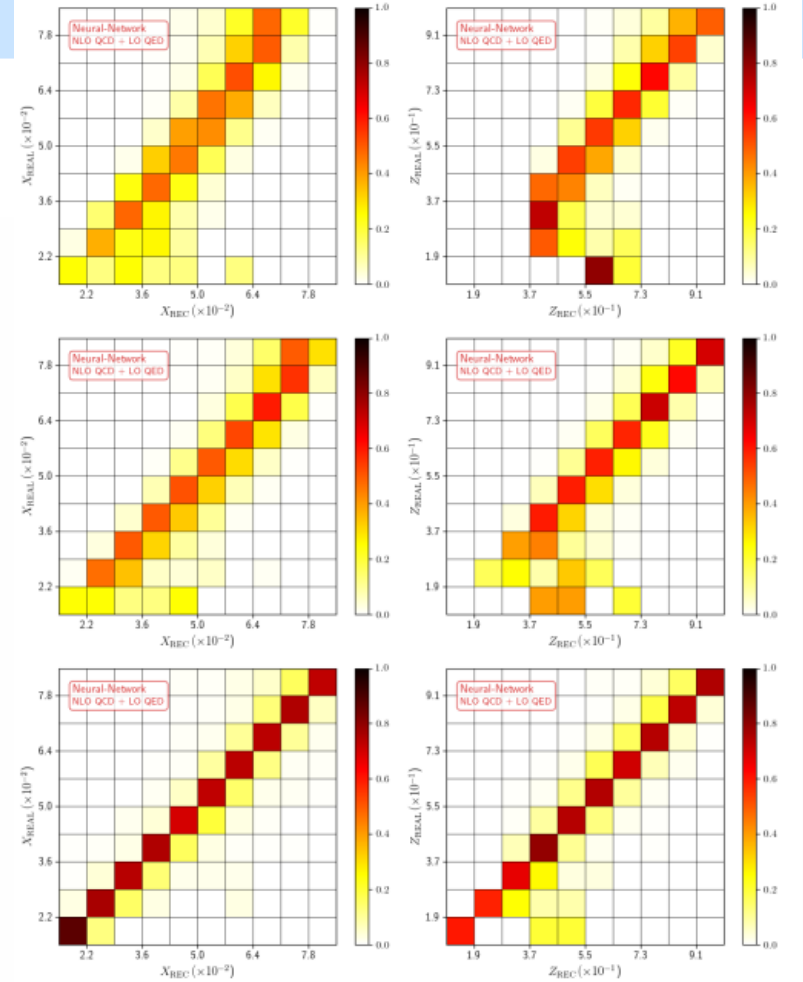


Figure 19: Comparison of the momentum fractions  $X_{\text{REAL}}$  vs.  $X_{\text{REC}}$  (left) and  $Z_{\text{REAL}}$  vs.  $Z_{\text{REC}}$  (right) obtained with MLP at NLO QCD + LO QED accuracy. The parameters for TEST1 (upper row), TEST2 (middle row) and TEST3 (lower row) are given in Table 3.

	$X_{REC} \text{ (LO)}$	$Z_{REC} \text{ (LO)}$	$X_{REC} \text{ (NLO)}$	$Z_{REC} \text{ (NLO)}$
# of hidden layers	2	1	5	5
# of neurons/layer	200	100	300	300
activation function	ReLU	ReLU	ReLU	ReLU
# iterations	$1 \times 10^5$	$1 \times 10^5$	$1 \times 10^{12}$	$1 \times 10^{12}$
learning rate	$1 \times 10^{-3}$	$1 \times 10^{-3}$	$1 \times 10^{-4}$	$1 \times 10^{-4}$

Table 2: Architecture for the MLP best fit parameters for the reconstruction of the momentum fractions at LO in QCD:  $X_{REC}(\text{LO})$  and  $Z_{REC}(\text{LO})$  (second and third columns), and for the momentum fractions at NLO QCD + LO QED:  $X_{REC}(\text{NLO})$  and  $Z_{REC}(\text{NLO})$  (fourth and fifth columns).

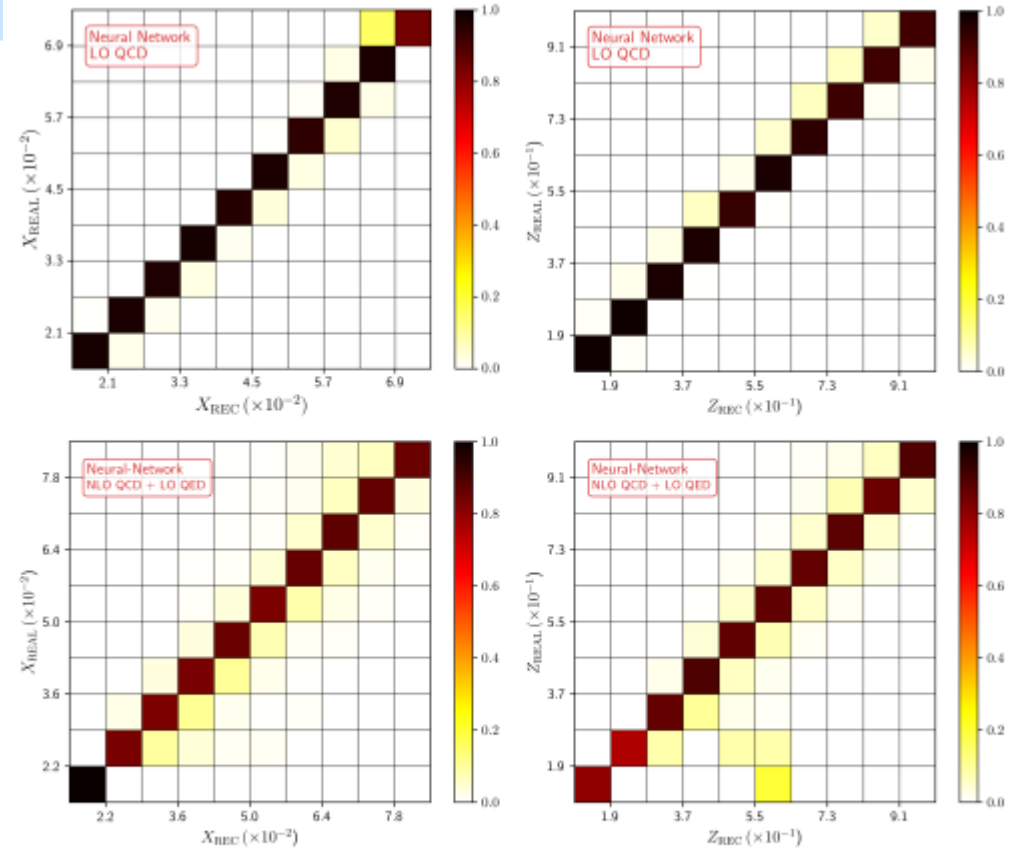
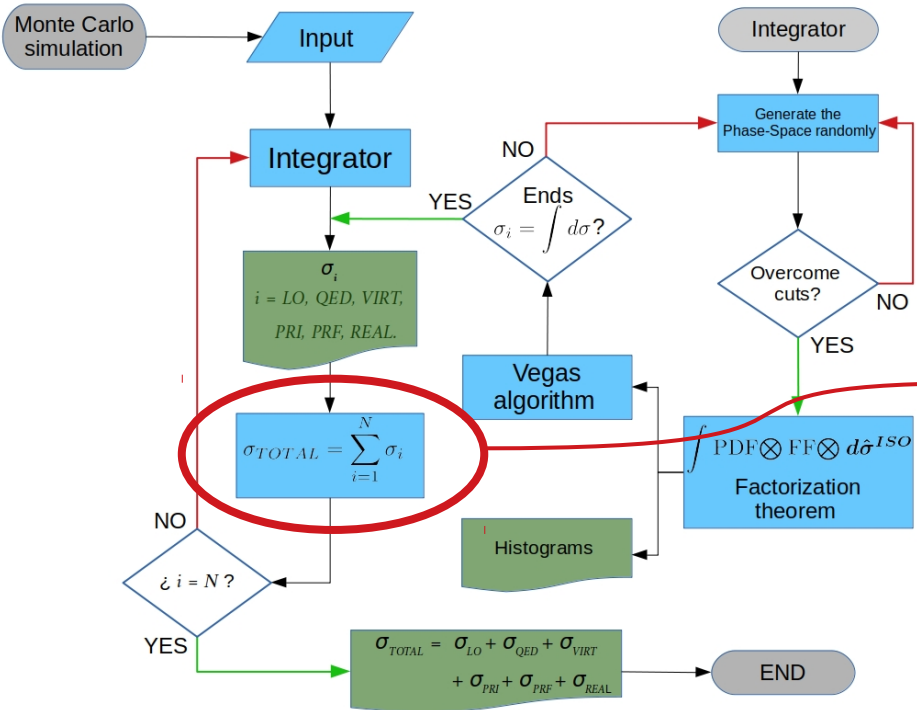


Figure 15: Left: Comparison of the momentum fractions  $X_{REAL}$  and  $X_{REC}$  obtained with MLP neural networks with the parameters given in Table 2. The upper (lower) row corresponds to the LO QCD (NLO QCD + LO QED) data set. Right: same as the l.h.s but for  $Z_{REAL}$  and  $Z_{REC}$ .

# Reconstructing the partonic kinematics

## Reconstructing $\{x, z\}$ at higher-order



- NLO corrections involve: real (2-to-3), virtual (2-to-2), counterterms (2-to-2).

- Create “bins” in the external variables and compute the cross-section:

$$p_j = \{\bar{p}_T^\gamma, \bar{p}_T^\pi, \bar{\eta}^\gamma, \bar{\eta}^\pi, \overline{\cos}(\phi^\pi - \phi^\gamma)\} \in \bar{\mathcal{V}}_{\text{Exp}}$$

$$\sigma_j(\bar{p}_T^\gamma, \bar{p}_T^\pi, \bar{\eta}^\gamma, \bar{\eta}^\pi, \overline{\cos}(\phi^\pi - \phi^\gamma)) = \int_{(p_T^\gamma)_{j,\text{MIN}}}^{(p_T^\gamma)_{j,\text{MAX}}} dp_T^\gamma \int_{(p_T^\pi)_{j,\text{MIN}}}^{(p_T^\pi)_{j,\text{MAX}}} dp_T^\pi \dots \times \int dx_1 dx_2 dz d\bar{\sigma}$$

- Weight the MC momentum fractions with the cross-section per bin:

$$(x_1)_j = \sum_i (x_1)_i \frac{d\sigma_j}{dx_1}(p_j; (x_1)_i)$$

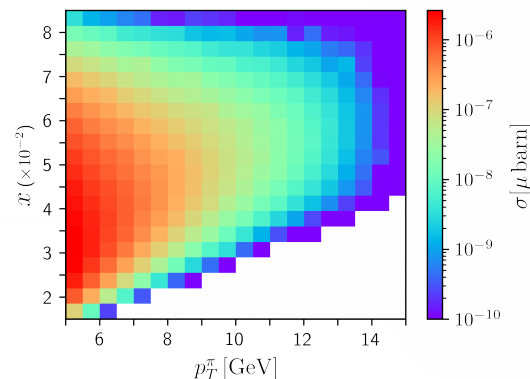
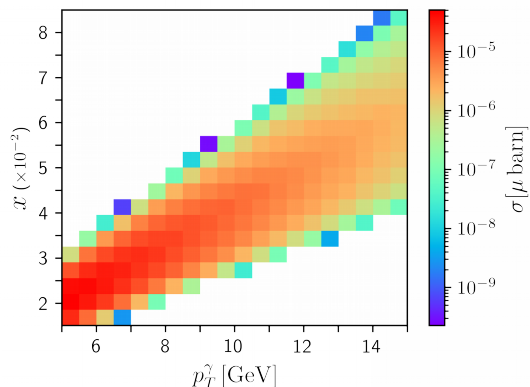
$$(z)_j = \sum_i z_i \frac{d\sigma_j}{dz}(p_j; z_i)$$

# Second: Photon + Hadron correlations

## LO kinematics

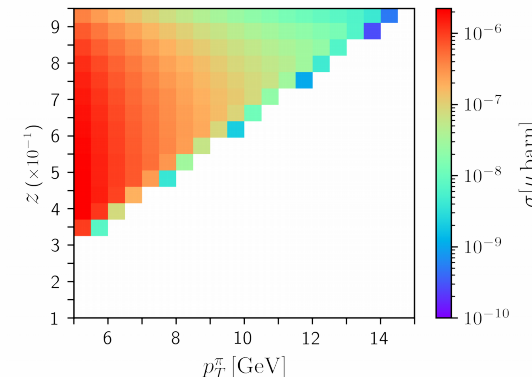
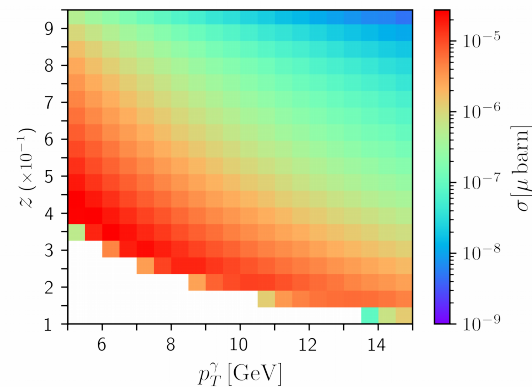
- $x$  vs  $p_T$

$$x_{1,2} = \frac{p_T^\gamma}{\sqrt{s}} \left( e^{\eta^{\pm\pi}} + e^{\eta^{\pm\gamma}} \right)$$



- $z$  vs  $p_T$

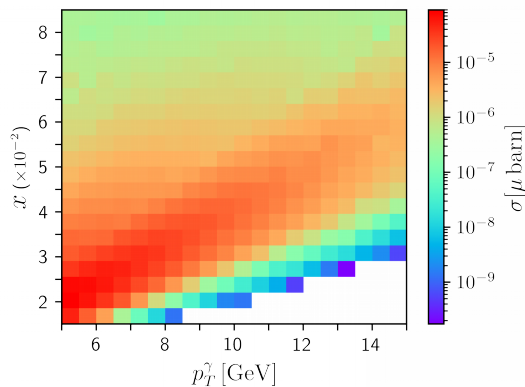
$$z = \frac{p_T^\pi}{p_T^\gamma}$$



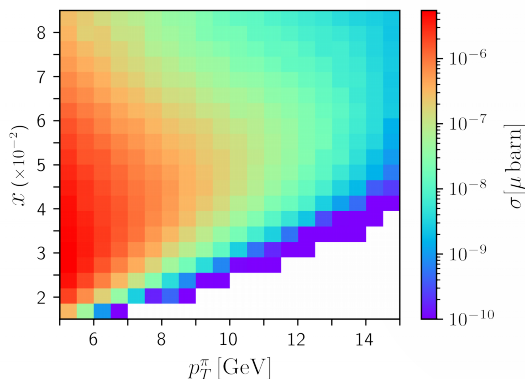
# Second: Photon + Hadron correlations

## NLO kinematics

- $x$  vs  $p_T$



$$x_{1,2} = ?$$



- $z$  vs  $p_T$

$$z = ?$$

